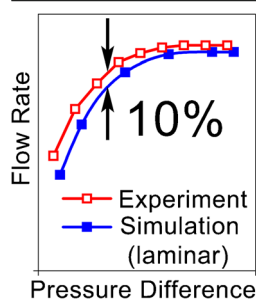RESEARCH ARTICLE

Gas Flow in the Capillary of the Atmosphere-to-Vacuum Interface of Mass Spectrometers

Michael Skoblin, [ORCID] Alexey Chudinov, Ilia Soulimenkov, Vladimir Brusov, Viacheslav Kozlovskiy

Institute for Energy Problems in Chemical Physics RAS (branch), Ac. Semenov prospekt 1/10 Chernogolovka, Moscow region, 142432, Russia

Abstract. Numerical simulations of a gas flow through a capillary being a part of mass spectrometer atmospheric interface were performed using a detailed laminar flow model. The simulated interface consisted of atmospheric and forevacuum volumes connected via a thin capillary. The pressure in the forevacuum volume where the gas was expanding after passing through the capillary was varied in the wide range from 10 to 900 mbar in order to study the volume flow rate as well as the other flow parameters as functions of the pressure drop between the atmospheric and forevacuum volumes. The capillary wall temperature was varied in the range from 24 to 150 °C. Numerical integration of the complete system of Navier-Stokes equations for a viscous compressible gas taking into account the heat transfer was performed using the standard gas dynamic simulation software package ANSYS CFX. The simulation results were compared with experimental measurements of gas flow parameters both performed using our experimental setup and taken from the literature. The simulated volume flow rates through the capillary differed no more than by 10% from the measured ones over the entire pressure and temperatures ranges. A conclusion was drawn that the detailed digital laminar model is able to quantitatively describe the measured gas flow rates through the capillaries under conditions considered.

Keywords: Atmospheric interface capillary, Numerical simulations, Viscous compressible gas flow, laminar flow

Introduction

Owing to development of atmospheric pressure ionization sources like electrospray and APCI (atmospheric pressure chemical ionization), mass spectrometers with atmospheric pressure ionization became more and more wide-spread. Ion transport from atmospheric pressure region into vacuum part of a mass spectrometer is often accomplished by a long capillary with inner diameter (i.d.) of the order of several tenths of millimeter and several centimeters long, which restricts the gas loading on the vacuum system of the device. The gas flow parameters have a critical effect on the ion transport in the capillary and are therefore of practical interest; many works are devoted to this subject. In [1], ion losses on the capillary walls due to space charge repulsion and ion diffusion were estimated and a qualitative influence of various peculiarities of gas flow in the capillary on the ion losses were discussed

without accounting for the real distributions of gas velocities and temperatures across the capillary. The ion motion through the capillaries of various shapes was studied in [2], using a specially designed experimental setup. Gas flow in the system was computed using the ANSYS package. After simulation, the resulting gas flow parameters were exported into the SIMION package. Using SIMION, the ion motion was simulated taking into account both gas dynamic and electric forces. In this work, the significant effect of gas dynamics on the ion motion in addition to the electrostatics was emphasized. The ion losses during ion transport through the bent capillaries were investigated experimentally in [3], focusing on the Dean-type secondary motion, a sort of gas circulation around the bent capillary axis, which led to the increase of ion loss. In [4], the numerical simulations of the gas motion in an asymmetric system consisting of a capillary and a non-coaxial skimmer were performed using both laminar and turbulent gas flow models. In that work, the conclusion was drawn that the main ion losses are defined by peculiarities of gas expansion at the exit of the capillary; at the same time, it was shown that only a

minor difference in simulated flow parameters was observed when the turbulent flow model was substituted by a laminar one. In [5], a set of capillaries with the same i.d. but different lengths were used to experimentally show that the gas entrainment was not the only force affecting the ions but both space-charge and ion diffusion play significant roles in ion losses inside the capillary. Many measurements of the air volume flow rate through capillaries of different lengths and i.d. were analyzed in [6], using various approximate analytic gas-flow models in pipes. In that work, an attempt was made to prove that the capillary flow under operation conditions of atmospheric interfaces must be turbulent. In [7, 8], the effectiveness of ion transport through the capillaries depending on the gas-flow conditions was investigated. A detailed numerical analysis of two-component flow (dry gas plus analyte gas) was performed in [9]. The most impressive part of that work was verification of the CFD results by direct particle image velocimetry (PIV) measurements.

Thus, a lot of experimental data on the gas flow in capillaries as well as a wide experience on gas-flow simulation of atmospheric interfaces have been accumulated so far. Nevertheless, the question of the underlying nature of such a flow is still open. Is the gas flow in a capillary under typical conditions of atmospheric interface laminar or turbulent? Appearance of a turbulent flow will influence ion transmission in the capillary by increasing the effective diffusion coefficient and changing the radial distribution of the velocities and temperatures inside the capillary. The notion of a turbulent gas flow in a capillary is based on Reynolds criterion, which was experimentally obtained for an incompressible liquid flow in a pipe (see [10] and references therein). Indeed, the mean flow velocities in the capillary approach the speed of sound for typical operation pressure drops between the capillary ends. The Reynolds number $Re = \rho \cdot V \cdot D/\eta$, where ρ is mean gas density, V is the gas velocity, D is the characteristic length scale of the system, and η is the gas dynamic viscosity, can reach several thousands. However, is a high value of Re a sufficient condition for a well-developed turbulence appearance for a given problem formulation? A detailed theoretical investigation of the stability of viscous compressible gas flow in a capillary at high Reynolds numbers is an extremely complicated computational task, which is out of the limits of this work. A good review of theoretical and experimental methods for investigation of transfer to turbulent conditions for water flow in pipes is given in [11].

In addition to a theoretical aspect, this question is of great importance from a flow modeling viewpoint as the direct numerical simulation of a turbulent motion is extremely complicated. When using semi-empirical turbulence models, the researches are faced with a boundary conditions problem. The point is that in order to apply one of the recently developed turbulence models (see, for example, [12, 13] and references therein) one has to solve an extra set of transport equations. For example, for the k–ε turbulent model [12], the transport equations for the turbulent kinetic energy k and its dissipation rate ε should be solved in addition to the usual set of Navier-Stokes equations. This means that at the simulation domain boundaries some special kind of boundary conditions are required for such parameters, and for them accurate measurements or even estimates could be a fundamental problem. The atmospheric interface of a mass spectrometer is a miniature device and detailed measurement of gas dynamic parameters inside it is a challenging task. Some integral quantities of a flow like volume flow rate through the system can be relatively easily measured in the experiments. Using an extended experimental setup, the temperature at the capillary walls, static pressure in the capillary, maximal gas velocity, and some other parameters can be measured [6]. However, these data are insufficient to estimate, for example, a mean value of the turbulent energy and its dissipation rate at the inlet boundary of the domain. Although the attempts of the direct experimental estimation of k near the inlet area of the transport capillary using the PIV instrumentation have been undertaken in [9], this method is too sophisticated to be widely used in practice. Hence, the practical choice of an adequate self-consistent turbulent gas motion model in agreement with experimental data is a very difficult task. A natural question arises then: whether or not it is possible to quantitatively describe the flow in the capillary, which is a part of the mass spectrometer atmospheric interface neglecting the turbulent component, i.e., assuming that the flow is laminar.

Despite of the apparent simplicity, the problem of a steady-state laminar flow of a viscous gas from the atmospheric pressure region into a forevacuum volume through an axially symmetric capillary of length L and i.d. R is rather complicated. For an adequate description of gas flow, the equations of motion of viscous *and* compressible gas should be solved [14]. The complete system of equations for this problem can not be solved analytically even for the simplest geometry (e.g.: cylindrical inlet volume - capillary - cylindrical outlet volume) and attempts to simplify the problem could lead to a complete loss of accuracy. The most thorough approach to this problem was developed in [14]. In that work, a subsonic gas flow was simulated using isothermal approximation and row expansions of the pressure and velocity components in terms of small parameters $\alpha = R/L$ and $\varepsilon = \Delta\rho/\rho$, were derived up to the second order. In a number of other works [6, 15, 16], the attempts to find a simple analytic solution were performed using much more crude assumptions. For example, substantially overestimated volume flow rates in comparison with experimental data were obtained in [6] using a simplified model of laminar flow in a capillary [15]. As a result it was concluded that the flow in the capillary certainly must be turbulent.

The aim of our work is to clarify whether the laminar model is suitable for description of air flow through the capillaries in atmospheric interfaces. For this purpose, we have performed numerical simulations of the viscous compressible gas flow taking into account the heat transfer. A simple model of the first stage of an atmospheric interface consisting of an inlet volume, a capillary, and an outlet volume was used. The simulation

results were compared with experimental data obtained in our laboratory and experimental data taken from [6].

Numerical Simulations

The design of the simulation domain, building the computational mesh and simulations themselves were performed within the framework of the gas dynamic package ANSYS CFX 15.0. As it will be shown in "Main Simulation Parameters" Section, the Knudsen number Kn equal to the ratio of the mean free path λ over the character length D (capillary diameter) is rather small for this problem ($Kn = \lambda/D << 1$), and that is why the continual Navier-Stokes approach is applicable for the flow simulation.

The physical flow model chosen in the data preparation module ANSYS CFX-Pre suggests simulation of a laminar high speed (both subsonic and supersonic) flow of an ideal viscous compressible gas (air) taking into account the heat transfer. The term «ideal gas» implies that it obeys the Mendeleev-Clapeyron equation of state, the viscosity and heat conductivity being the functions of the absolute temperature obtained by fitting the experimental data [17].

Steady-state solution was found using iterative approach with the time step $\Delta t = 0.5 \div 1.0$ µs so that the maximal Courant number ($Co = V \cdot \Delta t/\Delta x$, where Δx is the mesh edge size and V is the absolute velocity at a given point) was not greater than 10 in all our simulations. The solution convergence criterion was the decrease down to 10^{-3} of the maximal relative change of flow parameters computed over the entire domain for two successive iterations. The simulations had been carried out using the workstation with 16-kernel processor Intel Xeon 2.9 GHz. The mean solution convergence time was 8 h.

Simulation Domain and Boundary Conditions

The simulation domain consisted of three parts: auxiliary inlet volume, capillary, and auxiliary outlet volume. The auxiliary volumes were needed for correct boundary condition setting because the exact values of pressure, directions, and absolute values of velocities were unknown at the inlet and outlet cross-sections of the capillary. The irregular three-dimensional mesh inside the simulation domain was built to meet the requirements of the solution accuracy. Inside the capillary the maximal cell size did not exceed 0.075 mm; in the inlet volume average cell size was 1.0 mm, the mesh gradually getting denser when approaching the capillary entry. In the vicinity of the capillary exit and in the regions outside the capillary, where the sharp gradients of the flow parameters were expected, the mesh was also dense and the mean cell size was about 0.1 mm. Downstream at the distance of about 20 capillary diameters the cells were gradually getting larger and reached their mean size of about 1 mm at the exit of the domain. As the flow is supposed to be laminar and symmetric with respect to the XY plane, the domain represents, in fact, only a half of the real three-

dimensional domain occupied by the flow. To resolve the velocity profile in the vicinity of capillary walls, 4–5 additional layers of flat cells were added there. The simulation domain and two-dimensional mesh in the symmetry plane in different parts of the domain are shown in Figure 1.

Boundary conditions of four types were set at the simulation domain boundaries. At the inlet cross-section of the auxiliary inlet volume, where the estimated values of gas velocity are small, the full pressure equal to $P_0 = 10^3$ mbar was set. In addition, the velocity direction was postulated to be normal to the cross-section plane. The gas entering the domain was suggested to have a room temperature $T_0 = 24$ °C. The side surface of the cylindrical inlet volume formed a wall with temperature T_0, through which the gas cannot penetrate, but along which it can freely slip without friction.

The capillary surface was assumed to be a wall, at which a constant temperature T_{WALL} was set. One of the most important boundary conditions on the capillary walls was the adherence condition, i.e., equivalence to zero of not only normal but also tangential component of the velocity.

In the outlet volume, the side and the end-wall surfaces were assumed to be open. This means that the gas can leave the domain and enter the domain through these surfaces. At these surfaces an average static pressure $P_1 < P_0$ was postulated, which was one of the most important input parameters of the model, and which was varied from simulation to simulation. If the gas enters the domain through the opening, it was suggested to have temperature T_0. An additional boundary condition at the open surfaces was entrainment, i.e., equality to zero of the velocity derivative in the direction to the surface normal.

On the symmetry plane XY there was a special boundary condition that required zero derivatives in the direction normal to the plane for any gas dynamic parameter φ: $\partial \varphi \ / \ \partial \overrightarrow{n} = 0$.

A full rest $\overrightarrow{V} = 0$ at atmospheric pressure P_0 and room temperature T_0 was taken as initial conditions for all the simulations.
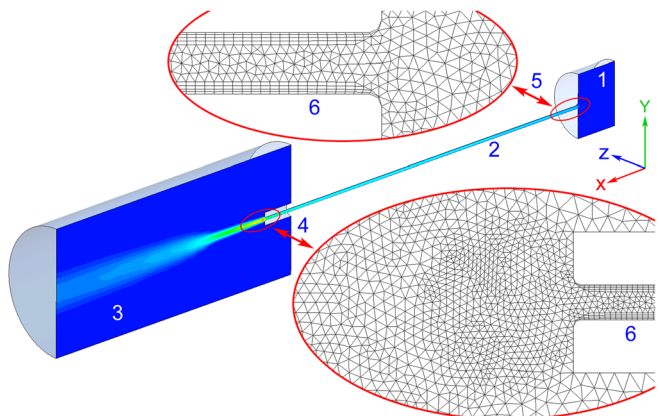

Figure 1. The simulation domain, boundaries, and mesh elements at the symmetry plane (the XY plane); 1 – inlet volume, 2 – capillary, 3 – outlet volume, 4 – 2D mesh at the XY plane near the capillary exit, 5 – 2D mesh near the capillary entry, 6 – additional prismatic layers

Table 1. Simulation Parameters

Capillary: diameter/length (D/L, mm)	0.5/60	0.6/60	0.5/58.5	0.58/58.5
Forevacuum pressure (P_1, mbar)	100 - 900	100 - 900	20 - 900	20 - 900
Capillary walls temperature (T_{WALL}, °C)	50, 150	27	24	24
Experimental data	[6]	[6]	Our experiments	Our experiments

Main Simulation Parameters

The capillary sizes, for which the simulations had been performed in this work as well as the forevacuum volume pressure ranges and capillary temperatures are presented in Table 1.

The capillary parameters, pressures and temperatures were chosen according to the experimental conditions used in [6] in addition to conditions of experiments carried out in our laboratory.

Experiment

The relationship of volume flow rate through the capillary versus the pressure in the forevacuum volume was studied using a simple experimental setup (Figure 2). The capillary outlet was opened into a big volume (3), which was pumped out by a forevacuum pump (5). The pumping rate was controlled by a valve installed into a forevacuum pump line. The pressure in the outlet volume was measured using the INFICON IR090 pressure gauge (4). The gas flow rate through the system was measured at the outlet of the forevacuum pump by a drum-type flowmeter GSB-400 (7), in which the gas, passing through a water-filled tank, rotated a measuring drum. The measurements were carried out at the room temperature equal to 24 ± 3 °C.

Results

After the steady-state solution had been obtained the simulation result file was loaded into the ANSYS CFD-Post 15.0 module, in which calculations of the volume flow rate through the capillary are performed in addition to calculations of other flow
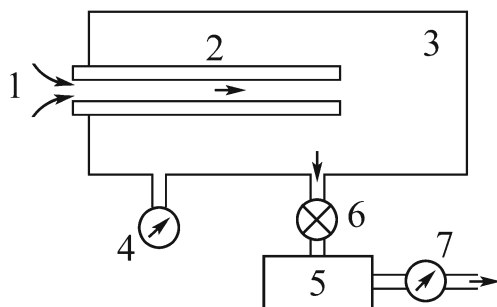

Figure 2. Experimental setup for the gas flow rate measurements; 1 – air inlet at one atmosphere, 2 – capillary, 3 – outlet volume, 4 – pressure gauge, 5 – forevacuum pump, 6 – pumping rate control, 7 – flowmeter

parameters both along the capillary axis and in cross-sectional planes.

Volume Flow Rate Through the Capillary

The dependencies of volume flow rate through the different capillaries versus the pressure difference between the atmospheric and forevacuum volumes are shown in Figure 3. The volume flow rate in our simulations was obtained from the mass flow rate by reducing it to the room conditions $T = 20$ °C, $P = 10^3$ mbar; the air density at these conditions was assumed to be equal to $\rho = 1.20$ kg/m^3.

It should be noted that for comparison of measured and simulated volume flow rates in the case of heated capillary (Figure 3a, b) experimental data [6] for the metal capillary had been chosen. This had been done because the heat conductivity of metal is substantially higher than that of glass, and one could expect that the constant temperature conditions at the *inner* surface of the capillary set in the simulations would meet better the temperature measured at the *outer* surface of the capillary.

Despite the difference between simulated and experimental flow rates reaching 20% at low values of the pressure differences ΔP (Figure 3c), the general agreement between our simulation results of the laminar flow and the experimental data is much better than that pointed out in [6] where the gas flow in the capillary was computed using simplified parametric models for both laminar and turbulent cases [15, 16]. The fact that the simulated curve in Figure 3d obtained for the capillary of nominal 0.5 mm i.d. lies in general by 10% lower than the experimental one could be explained by an inaccuracy of the capillary diameter measurement.

From comparison of the experimental and simulated flow rates for the same capillary size but for different capillary surface temperatures shown in Figure 3a, b, it is seen that the detailed numerical modeling of the laminar flow adequately describes the flow rate decrease for the enhanced temperature. When the capillary walls temperature was increased from 50 °C to 150 °C, the simulated volume flow rate decreased from 1.17 L/min down to 0.92 L/min in good agreement with the experimental data. In contrast to our simulations, the simplified flow models give wrong qualitative relationship between the capillary temperature and the flow rate through the capillary as it was pointed out in [6].
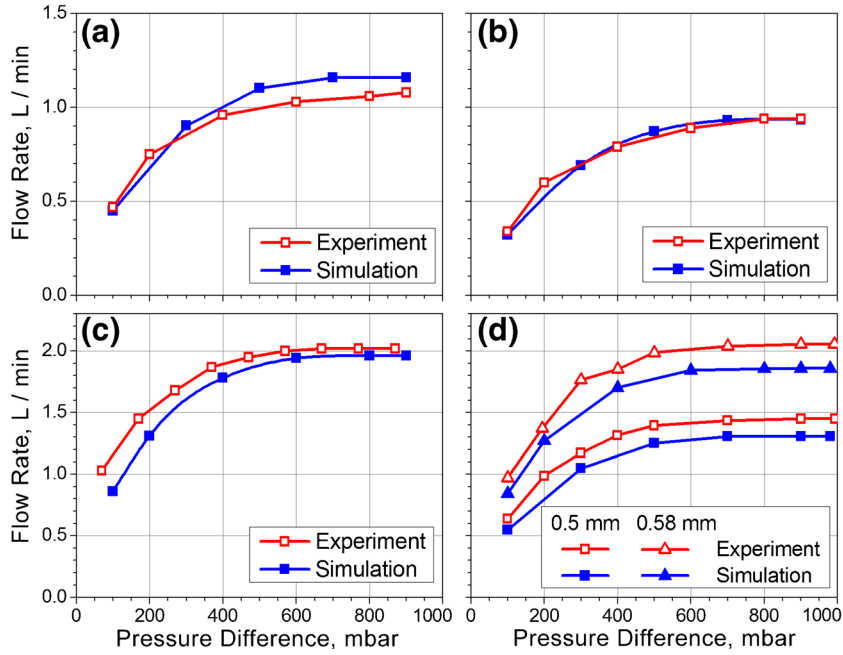
Figure 3. Simulated and measured volume flow rates through the capillaries versus the pressure difference ΔP. Red points and lines – experimental data; blue – simulations, ANSYS CFX. **(a)** – $D = 0.5$ mm, $L = 60$ mm, $T_{WALL} = 50$ °C; **(b)** – $D = 0.5$ mm, $L = 60$ mm, $T_{WALL} = 150$ °C; **(c)** – $D = 0.6$ mm, $L = 60$ mm, $T_{WALL} = 27$ °C; **(d)** – $L = 58.5$ mm, $T_{WALL} = 24$ °C. Experimental data on panels **(a)**, **(b)**, **(c)** are taken from [6], data on panel **(d)** are obtained in our experiments. Flow rate values are reduced to room conditions ($T = 20$ °C, $P = 10^3$ mbar, $\rho = 1.2$ kg m^{-3})

Reynolds Number in Capillary

In this work, we hold on to the traditional definition of the Reynolds number, although we express the cross-section averaged flow velocity u and density ρ via the mass flow rate W, which remains constant through any cross-section of the capillary:

$$\text{Re} = \frac{\rho\ u\ D}{\eta} = \frac{W \cdot 2R}{\pi\ R^2\ \eta} = \frac{4W}{\pi\ D\ \eta}, \tag{1}$$

where η stands for a cross-section averaged dynamic viscosity. The simulated Re versus ΔP relationships for all the cases listed in Table 1 are shown in Figure 4.

The Reynolds numbers plotted in Figure 4 had been computed for a cross-section located in the middle of the capillary, at a distance $x = 30$ mm from the capillary entry. It is seen that these values are pretty high, in particular for the capillaries with i.d. of 0.6 mm. By virtue of the criterion $\text{Re} > \text{Re}_C \approx 3500$, pointed out in review [11], for transfer of the viscous incompressible liquid flow in a pipe to the turbulent condition, one could conclude that there should present a well-developed turbulence in the capillary flows considered. Nevertheless, the results of volume flow rates computation (Figure 3) show that the laminar simulations result in good agreement with the experiment. This close coincidence of the simulations and the measurements makes us suggest that in case of capillary flows of the viscous compressible gas some higher value of the threshold Re_C could serve as a turbulence transfer criterion.

Flow Parameters Distribution Along the Axis

To study the distribution of various flow parameters at the axis of the system, we have chosen the case of metallic capillary with diameter $D = 0.5$ mm and length $L = 60$ mm, heated up to the temperature $T = 50$ °C. The volume flow rate through the capillary versus ΔP for this case is plotted in Figure 3a. Distributions of the simulated Knudsen number, Mach number, static pressure, axial velocity, and static temperature at the axis for five different values of the pressure drop ΔP are shown in
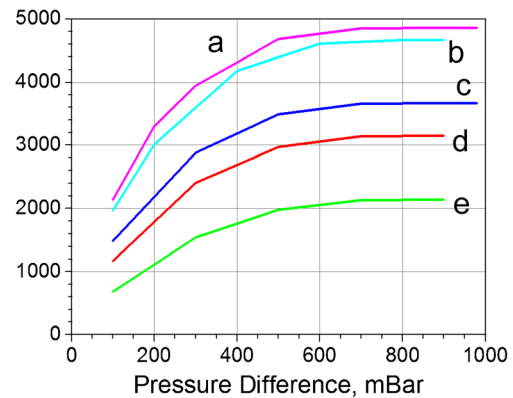

Figure 4. Simulated Reynolds numbers in the capillary versus the pressure difference ΔP. **(a)** – $D = 0.58$ mm, $L = 58.5$ mm, $T_{WALL} = 24$ °C; **(b)** – $D = 0.6$ mm, $L = 60$ mm, $T_{WALL} = 27$ °C; **(c)** – $D = 0.5$ mm, $L = 58.5$ mm, $T_{WALL} = 24$ °C; **(d)** – $D = 0.5$ mm, $L = 60$ mm, $T_{WALL} = 50$ °C; **(e)** – $D = 0.5$ mm, $L = 60$ mm, $T_{WALL} = 150$ °C

Figure 5. Note that for this capillary the entry and exit cross-sections were located at $x = 0$, and $x = 60$ mm, respectively.

It can be seen that the Knudsen number in the capillary did not exceed $Kn < 0.001$ so that the continuous medium Navier-Stokes equations can be used for the flow description.

The Mach number dependence on the axial coordinate (Figure 5b) shows that in the major part of the channel the flow is subsonic, even for the highest pressure drops, which is in full agreement with a known gas dynamic theorem stating that the transition to the supersonic velocities is impossible in the constant cross-section channel [18]. It should be noted that the last statement does not hold true for very rarified flows with $Kn \sim 1$ [19]. Starting with $\Delta P = 700$ mbar the gas velocity reaches the speed of sound in the vicinity of the exit cross-section (the radial velocity component becomes noticeable here, so that the flow is no longer strictly axial). This result is also in agreement with the statement of one-dimensional gas dynamics that the supersonic flow can be achieved when the pressures ratio is greater than approximately 2: $P_1/P_0 > 1.89$, (see [20], p. 706).

It seems to be interesting to consider the static pressure dependence on the axial coordinate x in more detail. From the approximate solution of motion equations for a compressible gas in a cylindrical pipe of radius R ([15], the laminar case) it is easy to get the following law of the static pressure variation with x:

$$P(x) = P_0 \left(1 - \alpha \cdot \frac{x}{L}\right)^{1/2}, \tag{2}$$

where $\alpha = 1 - (P_1/P_0)^2$. Functions (2) are plotted in Figure 5c for the same five values of the pressure drop $\Delta P = P_0 - P_1$ as for the rest plots; note the smooth character of the approximate solution $P(x)$. The numerical solution plotted in Figure 5d, however, shows that just after entering the capillary the pressure suddenly drops, and only after this drop the numerical relationship begins to be as smooth as (2). In addition, for high values of ΔP the numerical solution also reveals a short interval of pressure drop in the vicinity of the capillary exit. To investigate the reasons of such the pressure behavior, let us take
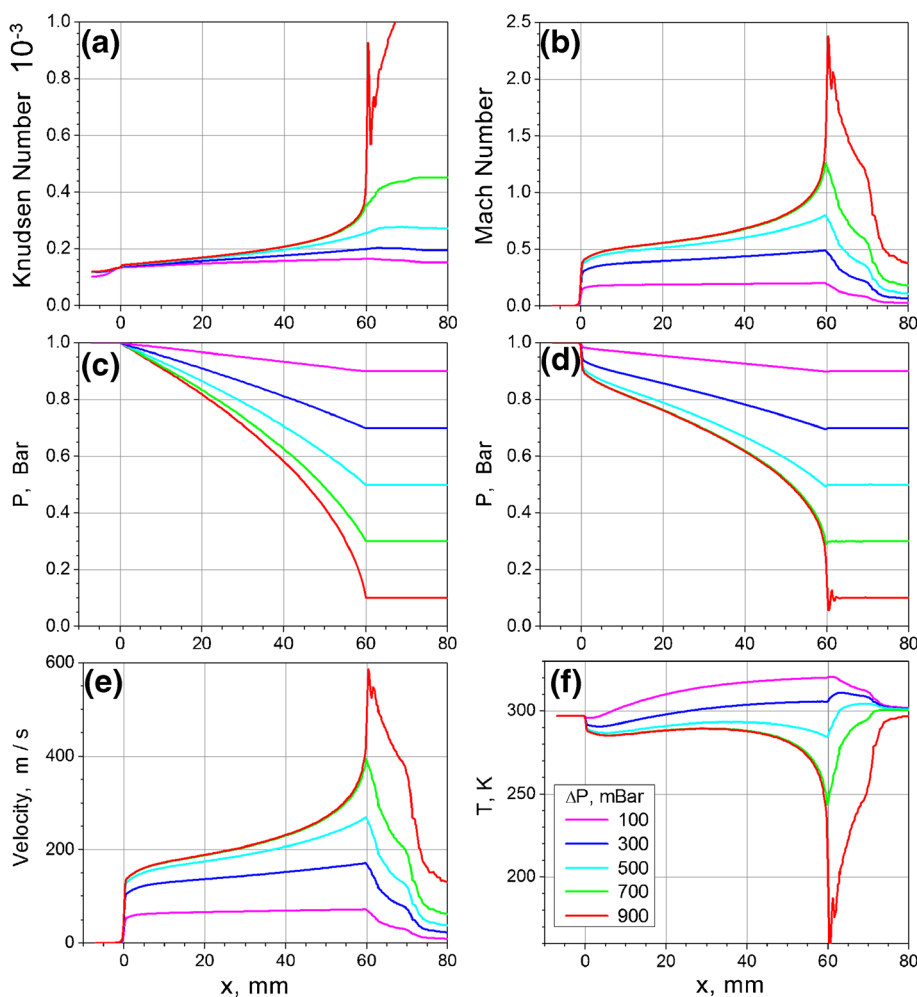

Figure 5. Flow parameters distribution at the axis of the system for different values of the pressure drop ΔP. **(a)** – Knudsen number, **(b)** – Mach number, **(c)** – static pressure (approximate expression (2)), **(d)** – static pressure (numerical solution), **(e)** – axial velocity, **(f)** – static temperature. Simulation parameters: $D = 0.5$ мм, $L = 60$ мм, $T_{WALL} = 50\ °C$

advantage of the computational abilities of the ANSYS Post package and analyze the terms of the momentum balance equation at the capillary axis. For the steady-state conditions and disregarding the volume viscosity the x-component of the Navier-Stokes equation looks like ([20], p. 200):

$$\left(\overrightarrow{V}\nabla\right) V_x = -\frac{1}{\rho}\frac{\partial P}{\partial x} + \eta\varDelta V_x + \frac{\eta}{3}\frac{\partial}{\partial x}\ divV. \qquad (3)$$

In expression (3) we have taken into account that the substantial derivative $\left(\overrightarrow{V}\nabla\right) V_x$ must stand for the x-component of gas acceleration in the steady-state flow conditions.

The terms of equation (3) at the capillary axis computed using numerical solution for the fields of velocity, static pressure, density, and dynamic viscosity for the case of $\varDelta P = 900$ mbar are plotted in Figure 6. The gas acceleration is shown by a red line, whereas blue and green lines designate the accelerating (pressure gradient) and retarding (viscous friction) forces. It is seen that the prominent surges of gas acceleration
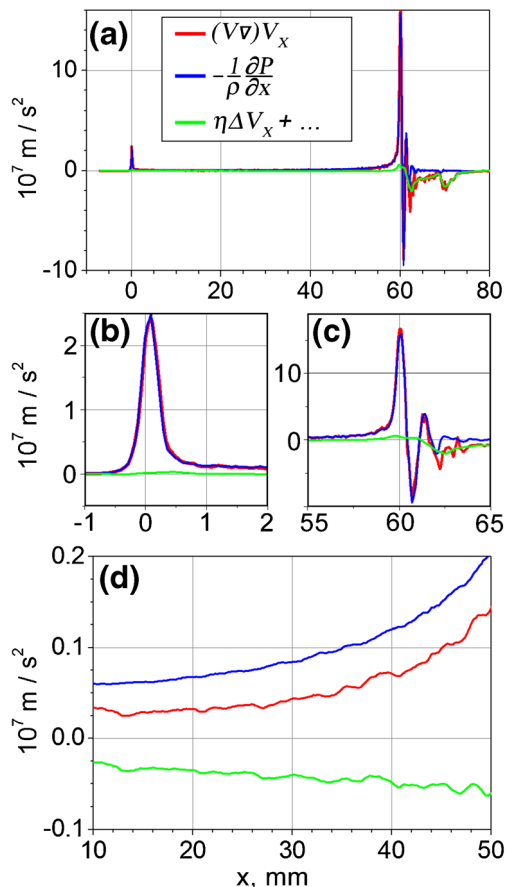

Figure 6. Terms of the x-component of the Navier-Stokes equation (3) at the axis of the system: **(a)** – in the whole capillary; **(b)** – in the vicinity of the entry cross-section $x = 0$; **(c)** – near the exit cross-section $x = 60$ mm; **(d)** – in the middle part of the capillary. $D = 0.5$ mm, $L = 60$ mm, the pressure drop $\varDelta P = 900$ mbar, the walls temperature $T_{WALL} = 50\ °C$

are localized at the capillary entry and exit cross-sections. Apparently, these surges could result from only sudden pressure drops (red and blue lines almost coincide) and the viscosity influence is negligible in these regions (Figure 6b, c). Far off the exit and entry cross-sections (Figure 6d) the gas is accelerated considerably slower, and its acceleration here is determined by balance between the pressure gradient and the viscous friction. Thus it becomes clear that the reason of fast static pressure drop at the capillary entry is the necessity to accelerate the gas from almost zero velocity in the inlet volume to velocities of the order of 50–150 m/s (Figure 5e). It is worth noting that the depth of the sudden pressure drop at the capillary entry is rather great: for $\varDelta P = 900$ mbar its value is about 10% of $\varDelta P$ itself. Apparently a similar situation takes place near the exit cross-section, at least for high pressure differences $\varDelta P \geq 700$ mbar, when the gas is accelerated in a short distance from approximately speed of sound to the speeds corresponding to the Mach number $M \sim 2.5$. It is interesting to note that similar pressure drop as well as the axial velocity increase in the vicinity of the inlet end of the capillary were obtained in [7] as a result of CFD simulations.

Thus our simulations show that the general difference between the simplified and the detailed numerical models of the gas flow through the pipes is in the boundary conditions setting. In the simplified models the values of static pressure are set exactly at the pipe ends. The flow immediately adjacent to the ends of the capillary is ignored, which results in a smooth dependence of the gas pressure and velocity on the axial coordinate, so that the gas accelerates gradually. Comparing the $P(x)$ curves in Figure 5c and d, one can see that neglecting the gas acceleration at entry and exit cross-sections of the capillary in the simplified model results in overestimated mean pressure gradient, which in its turn results in overestimated volume flow rates through the capillary. In our opinion, it was neglecting the parts of the flow just before and after the capillary that resulted in too high flow rates obtained in [6] with the help of simplified laminar flow model.

At low pressure differences $\varDelta P < 500$ mbar the relationship $P(x)$ becomes almost linear, and the depth of the local pressure drop near the capillary entry decreases. The axial distributions of the pressure at the axis for both simplified and numerical solutions become close.

The static temperature dependence on the axial coordinate at the capillary axis is also rather complicated (Figure 5f). The initial gas acceleration and expansion lead to a considerable temperature drop, up to $\varDelta T \sim 20K$, which is partly compensated later when the gas flows downstream due to radial heat transfer from the heated walls. The gas in the central part of the channel, however, can be heated only at quite moderate pressure differences $\varDelta P < 300$ mbar. When $\varDelta P$ increases, i.e., the flowing regime approaches the operational regime of the interface, the gas in the central parts of the capillary of $L = 60$ mm length is unable to heat, but on the contrary, cools due to a rapid expansion. Thus the numerical simulations show that gas flowing in the capillary is not heated homogeneously: in the vicinity of the walls gas has the wall temperature, and at the

same time the cold stream moves in the central part of the channel.

Discussion

The mass (or volume) flow rate through the capillary is one of the most important integral characteristics of the steady-state flow. When the pressure difference between the inlet and outlet volumes becomes sufficiently high, the flow rate becomes independent of the pressure in the forevacuum volume (Figure 3). The saturated flow rate, therefore, characterizes the gas conduction or throughput of a given capillary at a given wall temperature. As comparison of the terms of the momentum balance equation shows, in the major part of the capillary (Figure 6d) the pressure gradient is not so high as in the entry and exit cross-sections, and it is the viscous friction that restricts the gas acceleration and its velocity and, as a consequence, limits the flow rate. If the flow was fully turbulent, the momentum transfer in the radial direction would increase considerably, which would result in an effective increase of the viscosity. This effect is well known as the turbulent viscosity, or Boussinesq's hypothesis [12, 21]. The considerable increase of the viscosity coefficient should lead to the increase of the viscous friction force and, as a consequence, to the noticeable decrease of the flow rate through the capillary. It was more than 2-fold excess of the volume flow rates, computed using the simplified *laminar* flow model [15], over the measured flow rates that became in [6] one of the main arguments in favor of the turbulent flow hypothesis because the simplified *turbulent* models [15, 16] yielded lower flow rates and resulted in a better agreement with the experiment. Taking into account that the volume flow rate can be measured very accurately, we may state that the degree of agreement between the measured and simulated volume flow rates can serve as a good indicator of the validity of the flow model. As our simulations show, the volume flow rates computed using numerical solution for the detailed laminar model are in a very good agreement with the measurements (Figure 3). There is some underestimation (of about 10%) rather than overestimation of the flow rate in out simulations, which could probably be explained by 2%–3% inaccuracy of the capillary diameter measurement.

To emphasize the significance of the volume flow rate as an indicator of the presence or absence of the turbulent component in the capillary flow, it is worth drawing a parallel with incompressible liquid flow in a pipe and consider the Darcy friction factor (see, for example, [20], pp. 358–359). This dimensionless parameter characterizes the resistance of a pipe and for a smooth pipe depends on the Reynolds number only:

$$\frac{\Delta P}{\frac{1}{2}\rho V^2} = \frac{L}{D} \cdot f(\text{Re}). \tag{4}$$

Here V is the cross-section averaged velocity. The usefulness of (4) is that the empirical relationships $f(\text{Re})$ are quite general and have been obtained for both laminar and turbulent flows [20]. In the case of laminar flow $f(\text{Re}) = 64/\text{Re}$; when the flow is turbulent the relationship is more complicated. Essential for us is the fact that $f(\text{Re})$ is not continuous function of Re and that the turbulent branch of it lies remarkably higher than the laminar one. When Re increases the transition from laminar to turbulent regime occurs at some point depending on the conditions in the pipe but with inevitable increase of $f(\text{Re})$. For example, the plot presented in [20] shows that at Re = 3500 the friction factor must increase from ~0.02 to ~0.04 after a jump to the turbulent branch within the narrow transition zone. It is easy to see from expression (4) that the mass flow rate $Q = \pi R^2 \rho V$ is inversely proportional to the square root of $f(\text{Re})$, so that one could expect that the mass flow rate would decrease by a factor of $(0.04/0.02)^{1/2} \approx 1.4$ when the flow became turbulent. Returning to our results shown in Figure 3, we can see that both experimental and simulated volume flow rates are always non-decreasing functions of the pressure difference ΔP. In addition, expected flow rate drop related to a hypothetical transition to the turbulent regime (40%) is considerably greater than the flow simulation accuracy (10%) and the discrepancy between the experimental and simulated flow rates could be seen if the transition really took place. On the other hand, it seems to be obvious that at the low pressure end of our simulations the flow must be laminar as the Reynolds numbers there are pretty small 700 < Re < 2000.

Taking into account all the considerations above, we are led to a conclusion that there is no necessity to invoke the turbulent flow hypothesis to explain the measured volume flow rates.

Our results seem to be in agreement with [4], where detailed numerical simulations of the flow through a capillary with i.d. of 0.5 mm and length of 100 mm using both laminar and turbulent flow models had been performed. According to [4], velocities and temperatures at the end of the capillary differed for the two models no more than by 10% and 6%, respectively, and the difference in the mass flow rates did not exceed 3%. These results, in our opinion, confirm extremely low influence of the turbulent component on the flow under the conditions considered. It should be noted that using the k-ε-R_t turbulence model in [4] did not mean that a fully developed turbulence presents in the resulting flow. The k-ε-R_t model solves the transport equations for both turbulent kinetic energy k and its dissipation rate ε, boundary conditions for which (k_0 and ε_0) must be set at the inlet of the simulation domain. The permanent perturbations at the inlet, introduced by k_0 and ε_0, being transferred downstream, can either grow or decay, depending on the conditions in the fluid domain. Simulations performed in [4] indicate that the inlet perturbations do not turn into a fully chaotic turbulent flow but only lead to small deviations of flow parameters from those of the laminar case.

To support the statement of a well-developed turbulence in the capillary flow, special experiments were performed in [6]. The flow in the vicinity of the capillary entry was disturbed, which neither led to any significant flow rate variations nor resulted in ion transmission loss. This result was interpreted as if the flow was initially turbulent. However, these observations

can be interpreted quite the contrary. Indeed, if the flow in the capillary is stable the perturbations at the capillary entry will decay rather than grow and both flow rate and the ion transmission will not be affected.

To verify the validity of laminar or turbulent hypothesis one could compare also the temperatures predicted by the model and measured in the experiments. In [6], the difference ΔT between the mean flow temperature measured in the vicinity of the capillary outlet and the capillary walls temperature was numerically estimated using a combined model. Pressure $P(\overrightarrow{r})$ and velocity $\overrightarrow{V}(\overrightarrow{r})$ fields were calculated with the help of laminar isothermal model [14], and then the heat balance equation was solved within the Comsol Multiphysics package for the imported fields $P(\overrightarrow{r})$ and $\overrightarrow{V}(\overrightarrow{r})$. The calculated value of ΔT proved to be two times greater than the measured one, which was assumed to result from a considerable turbulent mixing presented in the real flow. In our opinion, there are two problems with such an interpretation. First, using the external pressure and velocity fields taken from the isothermal subsonic flow model for heat transfer simulation is not quite correct from the model self-consistency viewpoint. Second, measurements of the static temperature in a high speed gas flow are extremely complicated tasks. A gauge inserted in the flow inevitably distorts the flow pattern as it is, in fact, a still wall, at which the flow velocity falls to zero. That is why the result of measuring the gas temperature in a high speed flow by setting a micro-thermocouple into the flow as described in [22] is the stagnation temperature T_0, but not the static temperature T. When the Mach number M is known, the relationship between these values is given by the following expression [20]:

$$T_0 = T\left(1 + \frac{\gamma-1}{2}M^2\right). \tag{5}$$

Here $\gamma = c_P/c_V \approx 1.4$ is the adiabatic exponent for the air. To illustrate the difference between T and T_0 let us take a simulated flow in the capillary with i.d. $D = 0.5$ mm, length $L = 60$ mm, driven by the pressure difference $\Delta P = 900$ mbar, and with walls temperature $T_{WALL} = 50\ °C$ as an example. Figure 7 shows the static and stagnation temperatures distribution across two cross-sections, one located at $x = 60.3$ mm (out of the capillary) and the second one located at $x = 59.5$ (inside the capillary, 0.5 mm before the its exit cross-section). One can see that the stagnation temperature variations versus the y-coordinate across the section plane are quite small: T_0 varies within 20° in the flow downstream the exit cross-section and within 10° inside the capillary. The static temperature variations are much more pronounced. Inside the capillary at the $x = 59.5$ mm plane the static temperature is equal to the wall temperature in the vicinity of the walls ($T_{WALL} = 50\ °C$ in this example). When shifting in the direction to the capillary center, the static temperature drops, reaching the minimum $T = 240\ K$ at the very axis. The stagnation temperature at the axis is $T_0 = 320\ K$. It is easy to see that these values are in full agreement
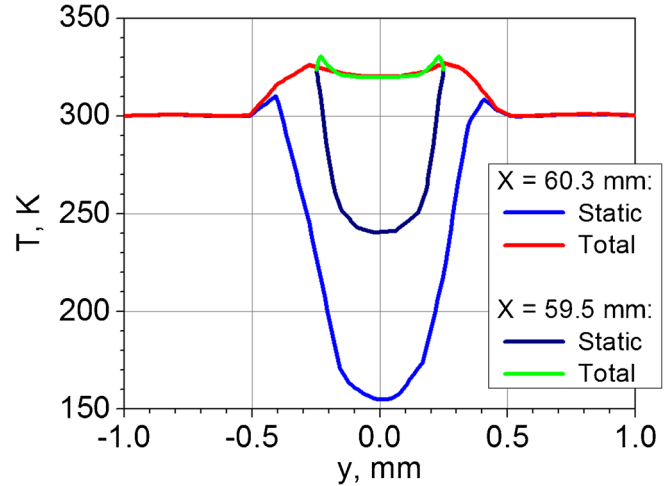

Figure 7. Stagnation temperature (Total) and static temperature (Static) versus the radial coordinate at two cross-sections: $x = 60.3$ mm (0.3 mm downstream the exit cross-section) and $x = 59.5$ mm (0.5 mm upstream the exit cross-section). $D = 0.5$ mm, $L = 60$ mm, the pressure difference $\Delta P = 900$ mbar, the walls temperature $T_{WALL} = 50\ °C$

with expression (5), if we take into account that the Mach number in this cross-section is $M = 1.3$ (Figure 3b, the red curve for $\Delta P = 900$ mbar). In the center of the other cross-section $x = 60.3$ mm the stagnation temperature is the same, but the static temperature proves to be still lower: $T = 150\ K$. This happens because the cross-section $x = 60.3$ mm is near the location where the flow velocity reaches its maximum, and the value of the Mach number here is nearly maximal $M = 2.4$. This example shows that the value of T_0 measured in the experiment can be several times greater than the static temperature, so that the comparison of the former with the static temperature obtained from the simulations is incorrect. In addition, if the heat transfer from the walls could be neglected, it is the stagnation temperature that would remain constant in the flow, but by no means the static temperature. Very probably, the stagnation temperature was meant when the conclusion was drawn that the flow in the capillary was "nearly isothermal." In fact, the experimental observation done in [6, 22] on the steadiness of the measured stagnation temperature supports our thesis about low efficiency of the gas heating by means of enhancing the capillary walls temperature because this observation fits with low radial heat transfer. Thus we are led to infer from all said above that there is not sufficient validation for strong turbulent mixing taking place in the capillary flow. There is also no evidence to support possibility of heating the high speed flow of gas in the capillary by heating only a short section of the capillary walls in the vicinity of its exit.

The strongest argument in favor of the turbulent character of the flow in the capillary is the high values of the Reynolds number exceeding the turbulent threshold $\mathrm{Re}_C = 3500$. It should be noted, however, that all the experiments on the turbulent threshold determination (see [10, 11] and references therein) were performed for an isothermal flow of a viscous incompressible liquid in pipes. The applicability of the

turbulence transition criterion obtained in such experiments to the capillary flow of the viscous compressible gas with heat transfer needs, at least, some validation. The Navier-Stokes equation for the compressible medium contains terms with $div\overrightarrow{V}$, which are absent in the case of an incompressible medium ([20], p. 200). This means that for the theoretical validation of the threshold Reynolds number in this case, the stability investigation for a different mathematical problem should be performed. To our knowledge, the stability of the viscous compressible flow with heat transfer with respect to finite perturbations was not investigated so far. That is why the applicability of the "traditional" criterion for such flow seems to be doubtful. There is another qualitative consideration, which casts doubts on the possibility of the well developed turbulence in the capillaries of typical atmospheric interfaces. The well developed turbulence appears due to growing of the perturbations inserted into the flow. First of such perturbations could be electrospray source. However, between such source and the high speed flow in the capillary there is a region in which the velocities are small and corresponding Reynolds numbers are much less than the threshold value Re_C. Such a region should serve as a sort of a damper for perturbations, which will decay before they enter the high speed part of the flow in the capillary. Another source of perturbations could be inner walls of either metallic or glass capillaries. However, they are manufactured smooth, so that the appearance of pertinent perturbations inside the capillary is unlikely. It is also very probable that due to the absence of strong perturbations, the flow in the capillary remains laminar even though the Reynolds numbers are far higher than the turbulence threshold. It is known from the classic experiments of Reynolds referred to in [11] that a laminar flow up to Re = 12,000 was observed. Certainly, all these qualitative considerations make sense only if the laminar flow model adequately describes the experimental data, as we just tried to demonstrate in this work.

Conclusions

Detailed numerical simulations of the laminar flow in the capillaries used in atmospheric interfaces of mass spectrometers had been performed for a viscous compressible gas (air), taking into account the heat transfer. The Navier-Stokes equation together with the continuity equation and the heat balance equation were solved using the standard gas dynamic package ANSYS CFX-15.0. The simulations were carried out for capillaries with i.d. of $R = 0.5\text{–}0.6$ mm and with lengths $L = 58.5\text{–}60$ mm for a wide range of the forevacuum volume pressure $P_1 = 10 - 900$ mbar and at room and enhanced temperatures of the capillary walls: $T_{WALL} = 24 - 150\ °C$. Comparison of the simulation results with the experimental data of [6] in addition to our experimental data had shown that the detailed numerical laminar model of the flow describes the dependence the volume flow rate on the pressure difference between the atmospheric and forevacuum volumes of the interface very well. At high values of pressure difference, i.e., in the regimes

close to the operation regime of a typical interface the difference of the simulated and measured volume flow rates did not exceed 10%. It was also shown that the detailed laminar model is able to quantitatively describe the dependence of the flow rate on the capillary walls temperature. The terms of the momentum balance equation at the capillary axis were analyzed using the numerical solution fields and the main reason of the difference between the simplified and numerical models in simulation the flow in the interface was proven to be in neglecting gas acceleration at the capillary entry and exit cross-sections in the simplified model. The static temperature pattern in the capillary flow was studied and the conclusion was drawn about a low efficiency of the gas heating in the high speed flow by increasing the walls temperature. In general, we conclude that the flow in capillaries under typical atmospheric interface conditions can be successfully described by a detailed laminar model of flow. It should be specially noted that we do not state that the flow in the capillary is fully laminar. It is very probable that the turbulent component of the flow is excited at the entrance of the capillary but then it decays rapidly and its influence on the gas flow rate under specific conditions of the atmospheric interface is small. Further investigations on ion dynamics in the capillary that take into account all possible mechanisms of ion losses (including space charge and molecular diffusion) are required to cast more light on the problem.

References

1. Lin, B., Sunner, J.: Ion transport by viscous gas flow through capillaries. J. Am. Soc. Mass Spectrom. **5**, 873–885 (1994)
2. Yu, Q., Jiang, T., Ni, K., Qian, X., Tang, F., Wang, X.: Experimental and simulation investigation of ion transfer in different sampling capillaries. J. Mass Spectrom. **50**, 1367–1373 (2015)
3. Chen, T., Xu, W., Garimella, S., Quyang, Z.: Study of the efficiency for ion transfer through bent capillaries. J. Mass Spectrom. **47**, 1466–1472 (2012)
4. Gimelshein, N., Gimelshein, S., Lilly, T., Moskovets, E.: Numerical modeling of ion transport in an ESI-MS system. J. Am. Soc. Mass Spectrom. **25**, 820–831 (2014)
5. Page, J.S., Marginean, I., Baker, E.S., Kelly, R.T., Tang, K., Smith, R.D.: Biases in ion transmission through an electrospray ionization mass spectrometry capillary inlet. J. Am. Soc. Mass Spectrom. **20**, 2265–2272 (2009)
6. Wißdorf, W., Müller, D., Brachthäuser, Y., Langner, M., Derpmann, V., Klopotowski, S., Polaczek, C., Kersten, H., Brockmann, K., Benter, T.: Gas flow dynamics in inlet capillaries: evidence for non laminar conditions. J. Am. Soc. Mass Spectrom. **27**, 1550–1563 (2016)
7. Pauly, M., Sroka, M., Reiss, J., Rinke, G., Albarghash, A., Vogelgesang, R., Hahne, H., Kuster, B., Sesterhenn, J., Kern, K., Rauschenbach, S.: A hydrodynamically optimized nano-electrospray ionization source and vacuum interface. Analyst **139**, 1856–1867 (2014)
8. Zhai, Y., Jiang, T., Huang, G., Wei, Y., Xu, W.: An aerodynamic assisted miniature mass spectrometer for enhanced volatile sample analysis. Analyst (2016). doi:10.1039/c6an00956e
9. Poehler, T., Kunte, R., Hoenen, H., Jeschke, P., Wissdorf, W., Brockmann, K., Benter, T.: Numerical simulation and experimental validation of the three-dimensional flow field and relative analyte concentration distribution in an atmospheric pressure ion source. J. Am. Soc. Mass Spectrom. **22**, 2061–2069 (2011)

10. Darbyshire, A.G., Mullin, T.: Transition to turbulence in constant-mass-flux pipe flow. J. Fluid Mech. **289**, 83–114 (1995)
11. Eckhardt, B., Schneider, T.M., Hof, B., Westerweel, J.: Turbulence transition in pipe flow. Annu. Rev. Fluid Mech. **39**(1), 447–468 (2007)
12. Launder, B.E., Spalding, D.B.: The numerical computation of turbulent flows. Comput. Methods Appl. Mech. Eng. **3**, 269–289 (1974)
13. Menter, F.R.: Two-equation Eddy-viscosity turbulence models for engineering applications. AIAA J. **32**, 1598–1605 (1994)
14. Venerus, D.C.: Laminar capillary flow of compressible viscous fluids. J. Fluid Mech. **555**, 59–80 (2006)
15. Wutz, M., Adam, H., Walcher, W. (eds.): Theory and practice of vacuum technology. Informatica International, Inc. Friedrich Vieweg & Sohn Verlagsgesellschaft mbH (1989)
16. Livesey, R.G.: Solution methods for gas flow in ducts through the whole pressure regime. Vacuum **76**(1), 101–107 (2004)
17. Gupta, R.N., Lee, K.P., Thompson, R.A., Yos, J.M.: Calculations and curve fits of thermodynamic and transport properties for equilibrium air to 30,000 K. NASA Report no. RP-1260. NASA Langley Research Center, Hampton (1991)
18. Szczeniowski, B.: Flow of gas through a tube of constant cross-section with heat exchange through the tube walls. Can. J. Res. **23a**, 1–11 (1945)
19. Raznikov, V.V., Zelenov, V.V.: New way to build a high-performance gas-dynamic interface to produce and transport ions into a mass analyzer. Int. J. Mass Spec. **325**, 86–94 (2012)
20. Fox, R.W., McDonald, A.T., Pritchard, P.J.: Introduction to fluid mechanics, 8th edn. Wiley, Hoboken (2011)
21. Schmitt, F.G.: About Boussinesq's turbulent viscosity hypothesis: historical remarks and a direct evaluation of its validity. C.R. Mecanique **335**, 617–627 (2007)
22. Klopotowski, S., Brachthäuser, Y., Müller, D., Kersten, H., Wissdorf, W., Derpmann, V., Brockmann, K.J., Janoske, U., Benter, T.: API-MS transfer capillary flow: examination of the downstream gas expansion. Proceedings of the 59th ASMS Conference on Mass Spectrometry and Allied Topics, Denver (2011)